CELL STRUCTURE AND FUNCTION 19: 349–362 (1994)

Flexural Rigidity of Echinoderm Sperm Flagella

Sumio Ishijima[1] and Yukio Hiramoto[2]

[1]Biological Laboratory, Faculty of Science, Tokyo Institute of Technology, O-okayama, Meguro-ku, Tokyo 152, and [2]Biological Laboratory, University of the Air, Wakaba, Mihama-ku, Chiba 261, Japan

Key words: beating plane/doublet microtubules/dynein cross-bridge/flagellar axoneme/stiffness/viscous resistance

ABSTRACT. **The stiffness (flexural rigidity) of live sperm flagella, Triton-demembranated flagella (axonemes), trypsin-digested axonemes, and doublet microtubules of the axonemes in echinoderms was determined from the relationship between their deformation when a stream of medium was applied and the viscous resistance of the medium acting on the flagellum. The stiffness of the flagellum beating in seawater was 5.8×10^{-21} Nm^2 for bending in the direction perpendicular to the beating plane and 4.2×10^{-22} Nm^2 for bending within the beating plane. A similar difference in stiffness from the difference in bending directions was found in reactivated flagella with 1 mM ATP. The stiffness of live flagella immobilized in CO_2-saturated seawater and axonemes in ATP-free medium was similar to that of beating flagella for bending in the direction perpendicular to the beating plane. The stiffness of motionless flagella significantly decreased with erythro-9-(2-hydroxy-3-nonyl) adenine (EHNA) and vanadate. The trypsin-digestion of motionless axonemes did not change their stiffness. The stiffness of doublet microtubules was 1.4×10^{-23} Nm^2 in 0.1 mM ATP medium and 6.1×10^{-23} Nm^2 in ATP-free medium. These results suggest that doublet pairs lying parallel to the beating plane of the flagellum retain fewer cross-bridges than doublet pairs lying perpendicular to the beating palne.**

In echinoderm sperm flagella, fairly planar bending waves are initiated at the base of the flagellum and propagate toward the tip. In the beating flagellum, the active bending force generated in it, the passive resistance due to the deformation of the internal structures, and the viscous drag of the external fluid applied to the flagellum are in balance with one another because the Reynolds number is very small (22). The measurement of mechanical properties of beating flagella is, therefore, important in the elucidation of the mechanism of flagellar movement. Baba (1) determined the flexural rigidity of compound cilia on *Mytilus* gill from the force applied to the beating cilium with a microneedle and the instantaneous change in the curvature of the ciliary shaft by the force. Okuno and Hiramoto (26) measured the stiffness of motionless echinoderm sperm flagella from the force applied to the flagellum with a microneedle and the bending of the flagellum caused by the force. They found that ATP decreases the stiffness of demembranated flagella and concluded that this reduction in stiffness was caused by the detachment of dynein arms from adjacent doublet microtubules. Okuno (25) investigated the effect of vanadate on the stiffness of demembranated flagella using the method of Okuno and Hiramoto (26) and found that the flagella are in a relaxed state in the presence of $MgATP^{2-}$ and vanadate.

In the present study, flexural rigidity was determined in echinoderm sperm flagella during beating and in a motionless state from the relationship between the deformation of the flagellum when the medium was moved and the viscous resistance of the medium acting on the flagellum. The effects of demembranation with Triton X-100, digestion of nexin links and radial spokes with trypsin, inhibition of dynein-ATPase with vanadate or erythro-9-(2-hydroxy-3-nonyl) adenine (EHNA), and the concentration of ATP on the flexural rigidity of the flagellum were also examined in order to investigate contributions of structures constituting the flagellum, such as cell membrane, doublet microtubules, nexin links, dynein arms, radial spokes, and central pair microtubules, to the flexural rigidity of the flagella during beating as well as during rest.

MATERIALS AND METHODS

Materials. Spermatozoa were obtained from the sand dollar, *Clypeaster japonicus*, and the regular sea urchin, *Pseudocentrotus depressus*, by intracoelomic injection of 10 mM acetylcholine dissolved in artificial seawater (ASW) (Jamarin U, Jamarin Laboratory, Osaka, Japan) for *Clypeaster japonicus* and by injection of 0.5 M KCl for *Pseudocentrotus depressus*. The obtained undiluted semen was stored in a refrigerator, and used within 2–3 hours after spawning. In the experiments

[1] To whom correspondence should be sent.

with live beating flagella, the semen was diluted to 10^5 times with ASW. To immobilize the sperm flagella, the semen was diluted to 10^3 times with ASW and then further diluted to 10^2 times with CO_2-saturated artificial seawater (CO_2-ASW). It was confirmed, after experimentation, that these immobilized spermatozoa recovered their motility when transferred to normal ASW (26). In some experiments, the sperm flagella ceased beating when transferred to ASW containing 2 mM erythro-9-(2-hydroxy-3-nonyl) adenine (EHNA) (Burroughs Welcome, Research Triangle Park, NC, USA). It was confirmed that the inhibition of flagellar motility by EHNA was reversed by 10 times dilution of the sperm suspension with normal ASW (3).

In experiments using demembranated spermatozoa, membranes of spermatozoa were removed according to the method of Gibbons and Gibbons (10) with minor modifications. One volume of sperm suspension prepared by 10^3 times dilution of the semen with ASW was mixed with 20 volumes of extraction solution (0.04% w/v Triton X-100, 0.15 M KCl, 4 mM $MgSO_4$, 0.5 mM ethylenediaminetetraacetic acid [EDTA], 0.5 mM dithiothreitol [DTT], pH 8.0 by 2 mM tris(hydroxymethyl)aminomethane [Tris]-HCl buffer). The mixture was gently agitated for 30 s at room temperature, and then the demembranated spermatozoa were diluted 50 times with reactivation solution (0.15 M KCl, 2 mM $MgSO_4$, 0.5 mM EDTA, 2 μM-1 mM ATP, 5 mM DTT, 2% polyethylene glycol [PEG, mol. Wt.=20,000, Nakarai Chemicals, Ltd., Kyoto, Japan], pH 8.0 by 20 mM Tris-HCl buffer). To inhibit ATPase activity of the demembranated flagella, the demembranated flagella reactivated with 1 mM ATP were put into the reactivation solution containing 10 μM sodium orthovanadate (Wako Pure Chemical Industries, Ltd., Tokyo, Japan) or 2 mM EHNA. After the measurements, the recovery of flagellar movement was checked by adding 2 mM norepinephrine (Sigma Chemical Co., St., Louis, MO, USA) to the medium in the case of the sperm flagella poisoned with sodium orthovanadate (7). In the case of the sperm flagella immobilized with EHNA, the recovery of flagellar activity was checked by diluting the medium 10 times with normal reactivation solution. The viscosity of ASW measured with an Ostwald's viscometer was 1.1×10^{-3} Pa.s and the viscosity of the reactivation solution and that of the ATP-free medium were both 2.5×10^{-3} Pa.s. Trypsin-digested demembranated flagella were prepared by treating the demembranated flagella with a solution containing 0.15 M KCl, 2 mM $MgSO_4$, 0.5 mM EDTA, 5 mM DTT, 2% PEG, 20 mM Tris-HCl buffer, pH 8.0, and 100 μg/ml trypsin (E. Merck AG, Darmstadt, Germany) for 5 min. Further digestion was stopped by adding an excess of soybean trypsin inhibitor (Sigma Chemical Co.). After the measurements, disintegration of the trypsin-digested demembranated flagella was checked by adding 1 mM ATP to confirm the digestion of the axoneme.

Broken segments of the axoneme were obtained by homogenizing the demembranated flagella. Doublet microtubules were obtained by treating these segments for 90 s with 100 μg /ml trypsin solution followed by exposure to 1 mM ATP following the method of Summers and Gibbons (30).

Observations and recording. The sperm suspensions were put in a trough (T in Fig. 1) on the stage of a microscope for observation. One of the spermatozoa was held by applying suction to its head with a braking micropipette (P), which had an inside diameter of approximately 1 μm and an outside diameter of approximately 4 μm at the tip (16, 17). The orientation of the spermatozoon was adjusted by tilting the micropipette attached to an instrument collar (I) held with a micromanipulator (M_1) (Ernst Leitz GmbH., Wetzlar, Germany) and rotating the micropipette on its axis so as to bring the entire length of the flagellum into the focal plane of the microscope. Since the micropipette was mounted in the instrument collar after passing through a hole (H) located on the axis of the instrument collar, the spermatozoon on the tip of the micropipette could be rotated within the microscopic field. The trough was moved on the microscope stage at a constant velocity with the operating head of an oil-pressure controlled micromanipulator (M_2; MO-102, Narishige Scientific Instrument Laboratory, Tokyo, Japan). The direction of movement was adjusted so as to be parallel or perpendicular to the main axis of the spermatozoon by rotating the stage of the microscope to which the operating head of the micromanipulator was fixed. The speed of the trough was controlled with one of two motors (D_1 and D_2), corresponding to x- or y-direction movement of the operating head attached to the control unit of the micromanipulator. The flow generated by moving the trough was nearly uniform even though there was a micropipette in the flow. The flow speed of the medium to which the flagellum was exposed was determined from the speed of several particles that were unaffected by the flagellar movement. Experimental error arising from this measurement is $\pm 20\%$. In experiments using motionless demembranated flagella treated with trypsin, EHNA, or vanadate, the proximal region of the flagellum (about 5 μm measured along the flagellum from the base) was sucked into the micropipette in order to provide firm support for its base.

Observations of the sperm flagella were made at 400× magnification with a Nikon phase-contrast microscope equipped with a 40× BM objective and a long-working distance condenser. For the microscopic observations, a high-pressure mercury arc lamp (Model HH 100T, Tiyoda Kogaku K.K., Tokyo, Japan) was used for illumination. For photographic recording, the flagellum was illuminated with stroboscopic xenon flashes at a rate of 200 Hz (Model 100, Chadwick-Helmuth Corp., El Monte, CA, USA). Images of the flagellum obtained by the microscope were then recorded with a Continuous Recording Camera (Model PC-2B, Nihon Kohden Kogyo Co., Ltd., Tokyo, Japan) on Kodak Tri-X film moving at a constant speed of 1 m/s, after appropriate magnification with the microscopic lens system.

The procedure for recording the bending of doublet microtubules by the medium stream was as follows. A drop of the suspension containing the doublet microtubules prepared as previously mentioned was put on a glass slide and covered

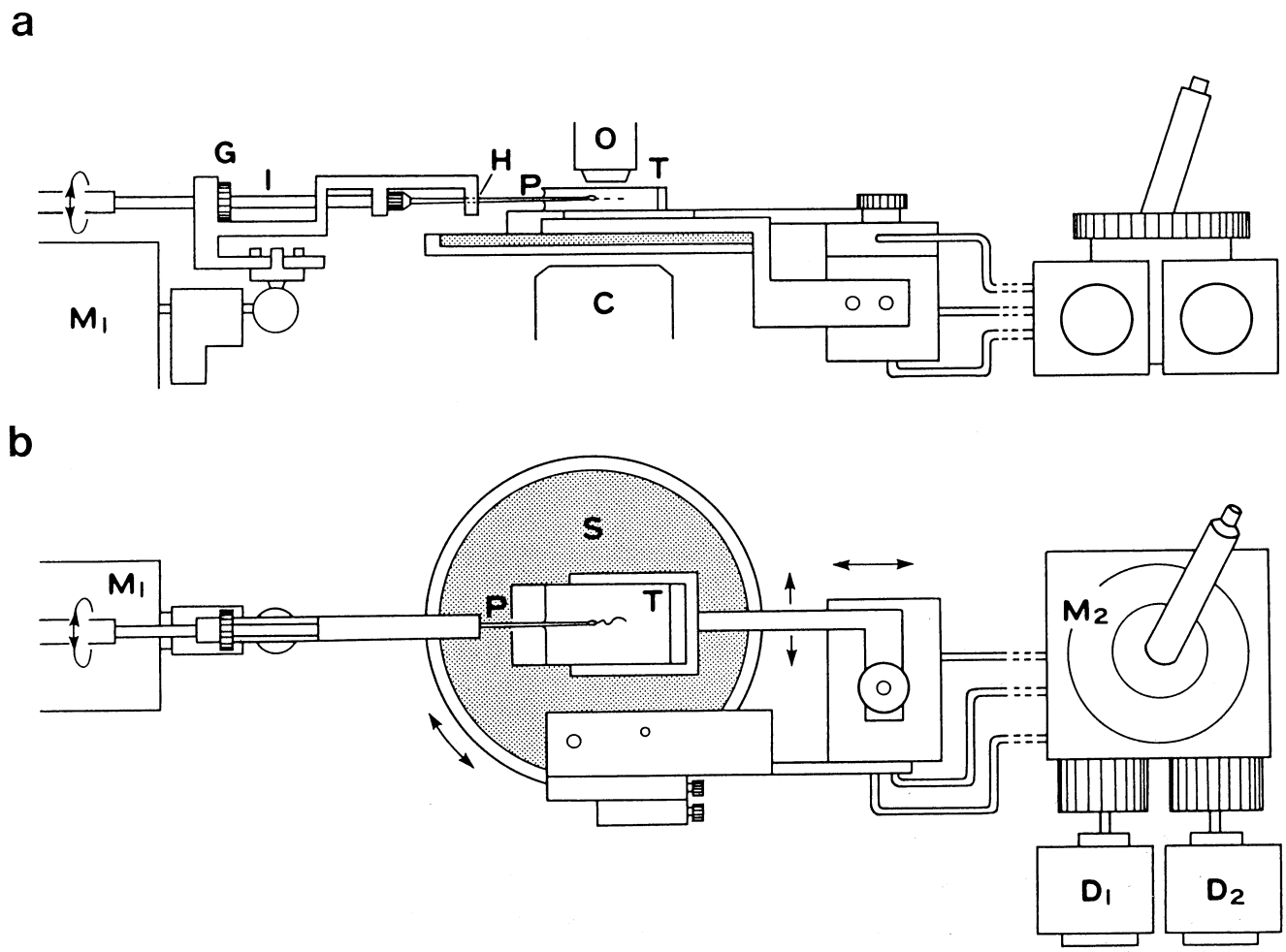

Fig. 1. Experimental setup. a, front view; b, plan view. C, long-working distance condenser; D_1 and D_2, motors; G, graduator measuring rotation angle of a micropipette; H, hole set on the axis of the instrument collar; I, instrument collar holding the micropipette; M_1 and M_2, micromanipulators; O, objective lens; P, micropipette; S, microscope stage; T, trough. See text for details.

with a coverslip so as to be in parallel with each other. The medium was made to flow by sucking the suspension with a strip of dry filter paper. The flow speed was determined from the speed of some particles occasionally passing through the vicinity of the doublet microtubules. Doublet microtubules attached to the coverslip at one end that were lying in a direction perpendicular to the flow were observed using a dark-field microscope equipped with a Nikon dark-field condenser and an Olympus oil-immersion objective (HI Apo 40/1.00). Microtubules in a still medium and in moving medium were recorded on 16 mm Kodak 4-X negative film with a 16 mm cinecamera (H 16M, Bolex International S.A., Yverdon, Switzerland) at 4 frames per second at 100× magnification with illumination from a high-pressure mercury arc lamp.

Analysis of the photographic records of flagella was carried out by tracing the image of the flagellum on a sheet of paper after 1,500× magnification with a photographic enlarger. Measurements were made directly on these traces. The curvature of the bend in flagella was measured by finding a circle fitting the trace of the bend from a set of template circles, with measurement error of ±30%.

Effects of stationary stream of the medium on the flagellar movement. During flagellar movement of echinoderm spermatozoa, bending waves are initiated at the base of the flagellum and propagate toward the tip. Since the bending of the flagellum occurs within a plane, the image of the flagellum that was in focus over its entire length could be observed by adjusting the beating plane so as to be perpendicular to the optical axis of the microscope (Fig. 2a).

When a stream was applied in the direction from the base to the tip of the flagellum, the wavelength of bending waves increased and the amplitude decreased as if the waveform was stretched in the direction of the stream (Fig. 2b), and as a consequence, the curvature of the bent portion of the flagellum de-

creased. When the speed of the stream reached a definite value (approximately 350 μm/s), the waveform rapidly became irregular (Fig. 2d), and a new bend was never generated in the flagellum above this value (Fig. 2e).

When a stream was applied in the direction from the tip to the base of the flagellum, the wavelength of bending waves decreased and the amplitude increased (Fig. 2c). When the speed of the medium increased in this direction, the curvature of the bend of the flagellum increased, though the curvature of the bend did not exceed a definite value (approximately 5×10^3 cm^{-1}; 2 μm in the radius of the curvature) as shown in Fig. 2f. When the stream speed exceeded approximately 200 μm/s, the wave was distorted and became nonplanar. Within the region approximately 5 μm from the base on the flagellum, the curvature of the bend of the flagellum was scarcely affected by the stream of the medium, suggesting that the flexural rigidity of the flagellum is larger in this region than in the remaining regions. As shown in Fig. 3, both the beat frequency and the number of waves contained in a flagellum were practically unchanged by the stream when the stream speed was smaller than a definite value (280 μm/s in the case of Fig. 3), whereas both the beat frequency and the wave number rapidly decreased when the speed exceeded this value. The effects of the medium stream on the waveform, the beat frequency, and the wave number were reversible; they recovered to their original values when the medium stream was stopped.

When the micropipette holding the spermatozoon was rotated by 90° on its axis to bring the beating plane of the flagellum perpendicular to the field plane of the microscope, parts of the flagellum in focus were observed as a train of spots moving toward the tip of the flagellum (Fig. 4a–c). When the medium was moved in the direction perpendicular to the beating plane, the beating plane was bent by the stream (Fig. 4a′–c′). The bending degree of the beating plane depended on the speed of the stream applied. When the speed of the stream was smaller than approximately 180 μm/s, parts of the flagellum observed in focus were continuously moving from the base of the flagellum toward the tip, indicating the propagation of the bending wave. In this case, the beat frequency was practically the same as the normal beat frequency. When the

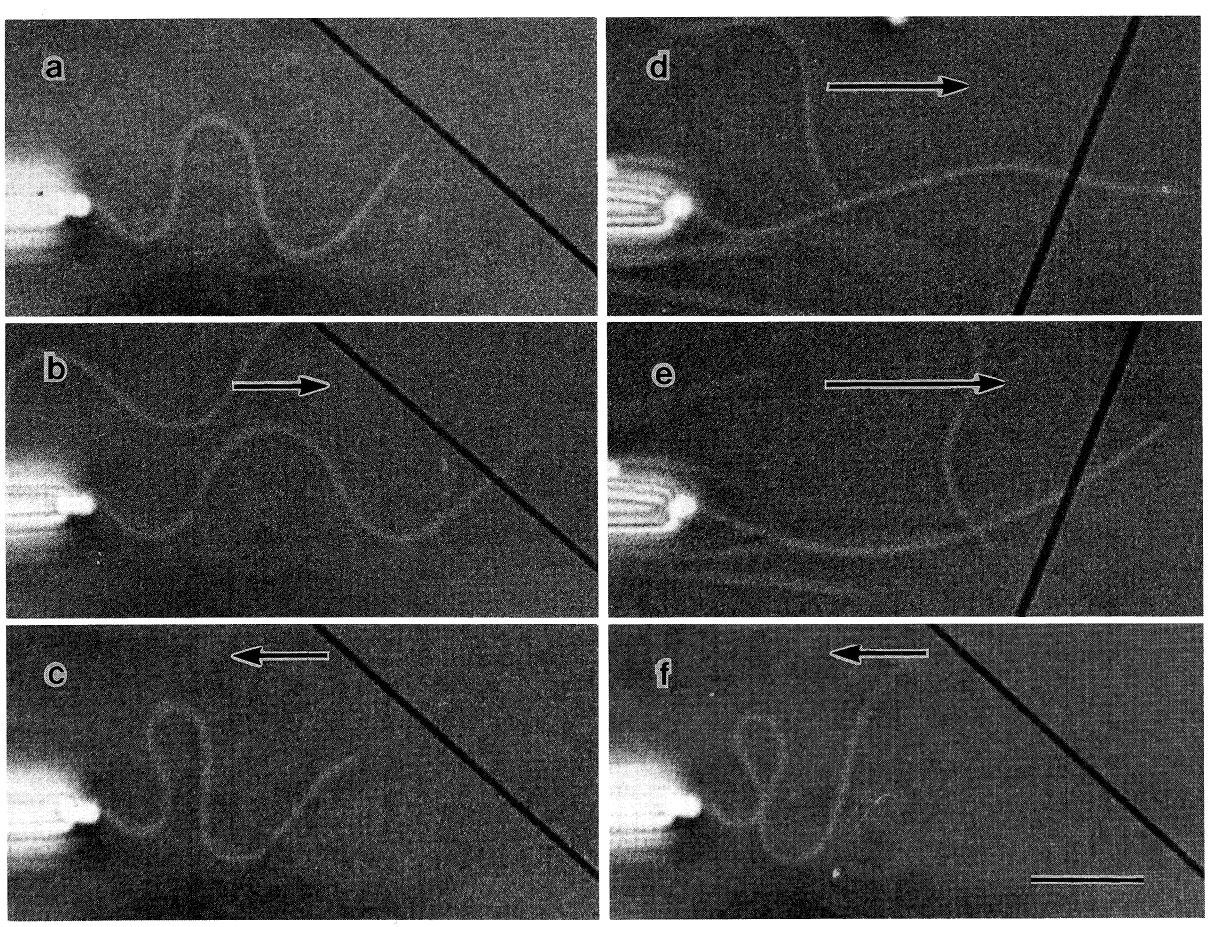

Fig. 2. Changes in the waveform of the flagellum of a sand dollar spermatozoon by a stream of medium. a, b, c, and f show the same spermatozoon, whereas d and e show another one. Arrows indicate the stream velocity: b, 170 μm/s; c, 140 μm/s; d, 350 μm/s; e, 400 μm/s; f, 160 μm/s. The scale bar represents 10 μm. See text for details.

speed of the stream was higher than approximately 180 μm/s, the bending wave was distorted and deviated from the regular curved plate. No difference in the bending degree was found between streams of opposite directions when the absolute values of the stream speeds were the same.

When demembranated flagella were put into the reactivation solution containing 1 mM ATP, they moved in a manner similar to that of live flagella (10). The effects of a stationary stream on the reactivated flagella were similar to those on live flagella: The bending wave was "stretched" when the medium stream was applied to the flagellum in the direction from the base to the tip of the flagellum and "compressed" when the stream direction was reversed, and the beating plane of the flagellum was bent when the stream was applied in a direction perpendicular to the beating plane.

Procedure for calculating flexural rigidity. The flexural rigidity of the beating flagellum was determined from the difference in the waveform of the beating flagellum between the moving medium and the still medium and the viscous resistance caused by the moving medium, assuming that the difference in the waveform of the beating flagellum is due to the elastic deformation caused by the viscous resistance of the moving medium.

The flexural rigidity of the motionless flagellum was determined from the relationship between the bending of the flagellum when its one end was held and the medium was moved at a constant speed, and the bending moment due to the viscous resistance of the medium acting on the flagellum. The same principle was used to determine the flexural rigidity of the demembranated flagella and the doublet microtubules.

The representation of the flagellar waveform by Fourier series. The waveforms of beating flagella in the absence of the stream, which were recorded by the previously described photographic techniques, were simulated by Fourier series in order to facilitate calculations of viscous resistance and viscous bending moments acting on the flagellum.

In each tracing of the image of beating flagellum at final magnification of 1500×, an orthogonal coordinate system, Oxy, was applied with the origin of the coordinate at the base of the flagellum and the x-axis as the straight line connecting the base of the flagellum to the tip. The segment of the x-axis between the origin and the tip, x_t, was divided into 12 equal-length portions and y-coordinates were measured for these 11 x-coordinate values. These y-coordinate values, y_i ($i=1, 2, 3, \ldots,$ and 11), were put in a calculator (41C, Hewlett-Packard Co., Corvallis, OR, USA) program that computed the values of the Fourier coefficients, a_k and b_k, using the following equation (35).

$$a_k = \begin{cases} (1/12)\sum_{i=1}^{11} y_i & \text{for } k=0, \\ (1/6)\sum_{i=1}^{11} y_i \cos(\pi/6)ik & \text{for } k=1, 2, 3, 4, 5, \\ (1/12)\sum_{i=1}^{11} y_i \cos \pi i & \text{for } k=6. \end{cases}$$

$$b_k = (1/6)\sum_{i=1}^{11} y_i \sin(\pi/6)ik \quad \text{for } k=1, 2, 3, 4, 5. \tag{1}$$

The waveform of the flagellum was represented by the Fourier series of the form:

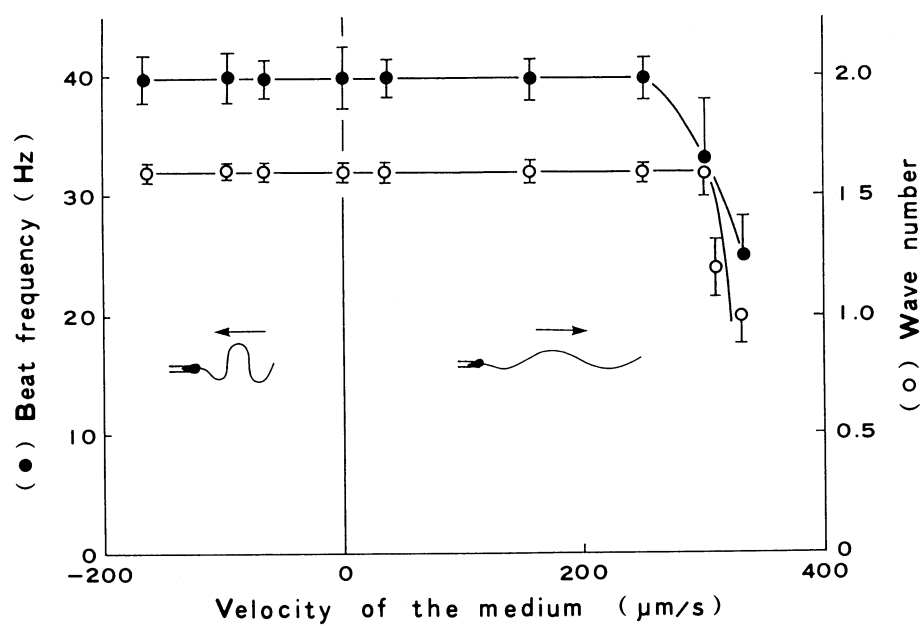

Fig. 3. Changes in the beat frequency and in the wave number of flagellar movement of a typical sea urchin spermatozoon at various medium speeds. Results from four measurements were averaged. Vertical bars represent standard deviations.

$$Y = \sum_{k=0}^{6} a_k \cos k\theta + \sum_{k=1}^{5} b_k \sin k\theta, \quad \text{where } \theta = 2\pi x/x_t. \tag{2}$$

This representation was used in each of the following calculations.

Calculation of the flexural rigidity for the bending within the beating plane. The waveform of the beating flagellum held by its head changed with the viscous resistance of the medium acting on the flagellum when the medium was moved par-

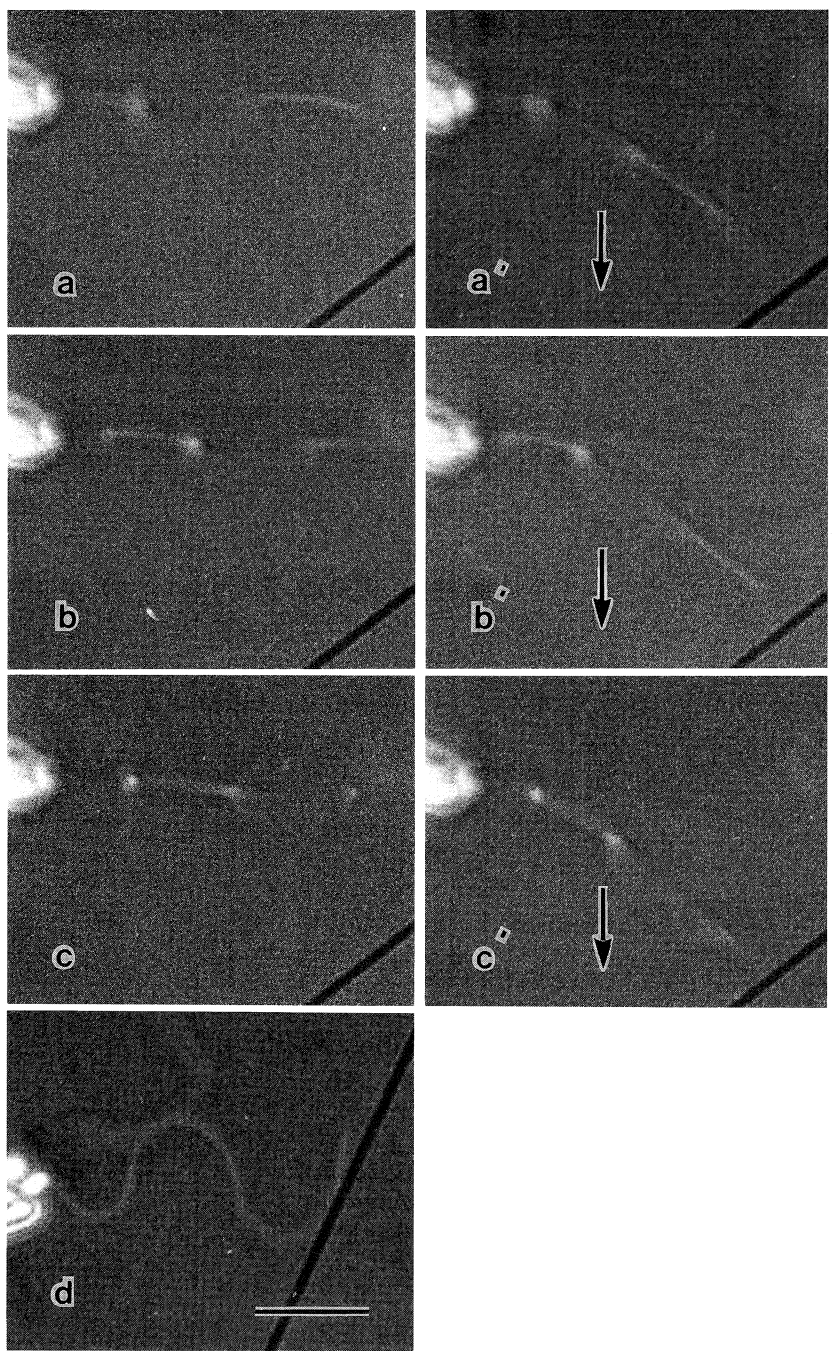

Fig. 4. Bending of the beating plane of the flagellum of a sand dollar spermatozoon due to medium movement. a, b, and c are successive images of flagellar movement observed from the direction of the beating plane at 1/200 s intervals. a′, b′, and c′ show beating planes of the same flagellum when the medium is moving in the directions shown by the arrows. The stream velocity is 150 μm/s. d shows the form of the same flagellum observed from the direction perpendicular to the beating plane. The scale bar represents 10 μm.

allel to the beating plane (Fig. 2).

Letting the equation simulating the waveform of the beating flagellum by Fourier series be $y=f(x)$ and letting the direction cosines of the tangent and the normal at any point, $Q(x,f(x))$, on the flagellum (Fig. 5) be **t** and **n**, respectively, where **t** and **n** are expressed as:

$$\mathbf{t}=(1/\{1+[f'(x)]^2\}^{1/2}, f'(x)/\{1+[f'(x)]^2\}^{1/2}),$$
$$\mathbf{n}=(-f'(x)/\{1+[f'(x)]^2\}^{1/2}, 1/\{1+[f'(x)]^2\}^{1/2}). \quad (3)$$

The position vector **R** directed from point $P(x_p,f(x_p))$ to Q is expressed as:

$$\mathbf{R}=(x-x_p, f(x)-f(x_p)). \quad (4)$$

The bending moment, dM, around point P due to the viscous resistance of the medium acting on a minute segment (length: ds) at point Q is given by

$$dM=dF_L(\mathbf{R},\mathbf{n})-dF_N(\mathbf{R},\mathbf{t}), \quad (5)$$

where dF_L and dF_N are the components of the viscous resistance ($d\mathbf{F}$) tangential and normal to the flagellar axis, respectively. According to Gray and Hancock (15), the tangential and the normal components, dF_L and dF_N, of the viscous resistance acting on the segment placed in a stream are expressed by

$$dF_L=(d\mathbf{F},\mathbf{t})=C_L V_L ds,$$
$$dF_N=(d\mathbf{F},\mathbf{n})=C_N V_N ds, \quad (6)$$

where V_L and V_N are the velocity components tangential to and normal to the segment axis, respectively. C_L and C_N are coefficients of resistance for movement to the segment along and normal to the axis, respectively. According to Lighthill (21), C_L and C_N for thin fibers such as flagella are obtained by

$$C_L=2\pi\mu/\ln(2q/a),$$
$$C_N=2\pi\mu/[\ln(2q/a)+0.5], \quad (7)$$

where a is the radius of the flagellum, $q=0.09\times l$ (where l is the wavelength measured along the flagellum), and μ is the viscosity of the medium. In the present study, the wavelength of the flagellar bending wave was in the range from 27 to 33 μm and the viscosity of each working solution was 1.1×10^{-3} Pa.s for ASW and 2.5×10^{-3} Pa.s for both the reactivation solution and the ATP-free medium. Substituting these values and the radius of the flagellum, $a=0.1$ μm, (32) into Eq. 7 gives approximately constant values for C_L and C_N: $C_L=1.5\times10^{-3}$ Pa.s and $C_N=2.7\times10^{-3}$ Pa.s for ASW and $C_L=3.8\times10^{-3}$ Pa.s and $C_N=6.8\times10^{-3}$ Pa.s for both the reactivation solution and the ATP-free medium. These values were used for C_L and C_N in the present study.

Substituting Eqs. 3, 4, and 6 into Eq. 5 and using $ds=\{1+[f'(x)]^2\}^{1/2}dx$ give the bending moment, dM,

$$dM=\{C_L V_L[(x_P-x)f'(x)+f(x)-f(x_P)] - C_N V_N[x-x_P+(f(x)-f(x_P))f'(x)]\}dx. \quad (8)$$

Expression of the components of the velocity, V_L and V_N, in terms of the x component (V_x) and y component (V_y) of the velocity (**V**) can be written as:

$$V_L=[V_x+V_y f'(x)]/\{1+[f'(x)]^2\}^{1/2},$$
$$V_N=[-V_x f'(x)+V_y]/\{1+[f'(x)]^2\}^{1/2}. \quad (9)$$

The total bending moment around point P on the flagellum, where the curvature was determined, is the sum of the moments due to the resistance acting on all segments distal to that point. Substituting Eq. 9 into Eq. 8 and integrating the bending moment, dM, from the tip of the flagellum to P gives the total bending moment, $M(x_P)$, around point $P(x_P,f(x_P))$ on the flagellum,

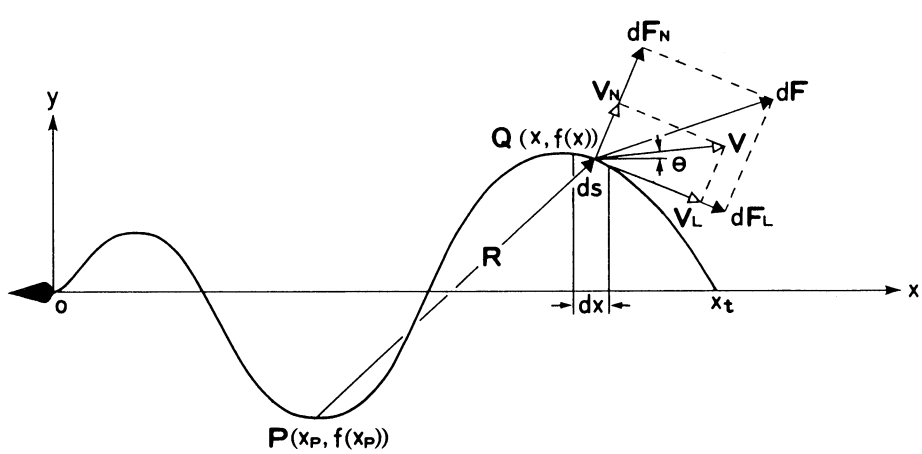

Fig. 5. Diagram illustrating parameters for calculation of forces and bending moments. See text for details.

$$M(x_P)=\int_{x_t}^{x} dM$$
$$=\int_{x_t}^{x} dx\{C_L[V_x+V_y f'(x)][(x_P-x)f'(x)+f(x)-f(x_P)]$$
$$-C_N[-V_x f'(x)+V_y][x-x_P+(f(x)-f(x_p))f'(x_P)]\}$$
$$/\{1+[f'(x)]^2\}^{1/2}. \quad (10)$$

The calculation was made by loading the program containing Eq. 10 into the calculator and inputting the data, the distance x_t from the base to the tip of the flagellum, and both speed, V, and the direction, θ, of the medium movement (Fig. 5). The integral in Eq. 10 was calculated with Simpson's 1/3 rule with 20 intervals (dx=1–2 μm). To test the accuracy of the numerical procedures, sine curves which had the same amplitude and wavelength as waves observed in sperm flagella were used. These curves were simulated by Fourier series and the resulting data processed as described above were compared with analytically calculated values. The errors inherent to the numerical procedures were negligible compared with the experimental errors (18, 28).

From tracings at a final magnification of 1,500×, the maximal curvature, K, of the bend at a point, which was approximately 20 μm from the base (P in Fig. 5), on flagellum beating in the moving medium and the maximal curvature K_0 of the bend of the same flagellum beating in still medium with the same beating phase were measured.

The flexural rigidity of the flagellum (S) was calculated by the following equation (20):

$$S=M(x_P)/(K-K_0), \quad (11)$$

where $K-K_0$ is the difference in curvature at point P between the flagellum beating in the moving medium and the flagellum in still medium.

Calculation of the flexural rigidity for the bending in the plane perpendicular to the beating plane. When the stream of the medium was applied in the direction perpendicular to the beating plane of the flagellum, the beating plane was bent by the stream (Fig. 4). The flexural rigidity for the bending in the plane perpendicular to the beating plane was determined by comparing the observed deformation with the deformation due to the bending and the twisting of the flagellum computed with the calculator using hydrodynamic theories and the waveform of the beating flagellum represented by the Fourier series.

When a flagellum is exposed to a medium stream flowing in the direction perpendicular to the beating plane, it is expected that the flagellum is bent and twisted by viscous resistance acting on the flagellum. In each tracing at a final magnification of 1,500× of the image of the beating flagellum, the origin of coordinates, 0, was placed at the base of the flagellum and the orthogonal coordinate system, Oxyz, with a straight line tan-

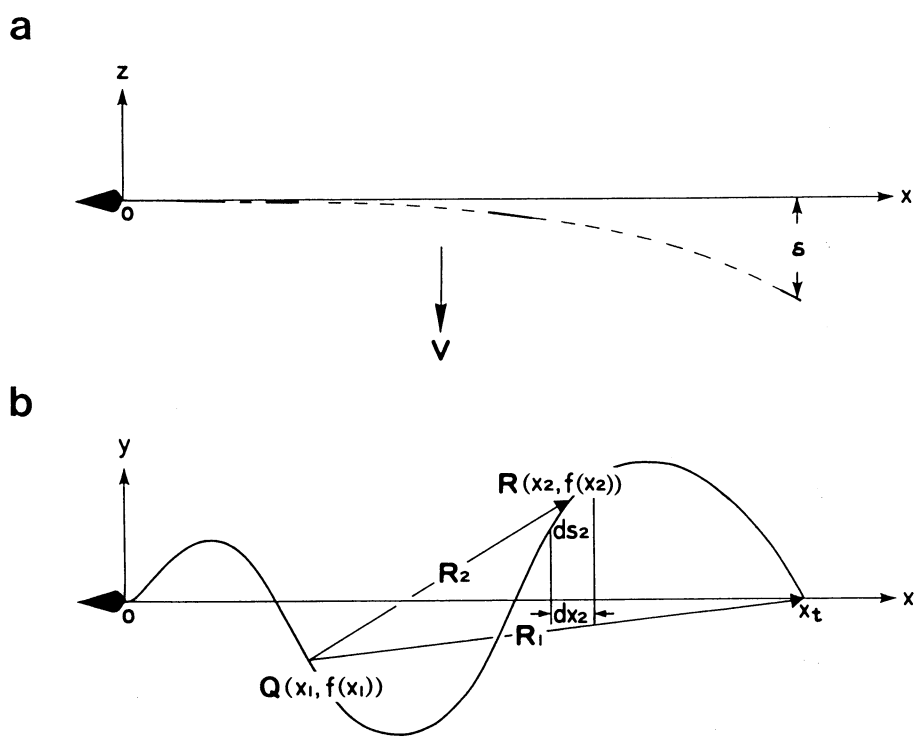

Fig. 6. Diagram illustrating parameters for calculation of the flexural rigidity for bending in the plane perpendicular to the beating plane. See text for details.

gential to the beating plane at the base of the flagellum and passing the tip as the x-axis, the y-axis in the beating plane, and the z-axis perpendicular to the x- and y-axes, was applied as shown in Fig. 6.

Letting the equation simulating the waveform of the beating flagellum using a Fourier series be $y=f(x)$, and letting the direction cosines of the tangent and the normal at point $Q(x_1,f(x_1))$ on the flagellum be $\mathbf{t}_1$, $\mathbf{n}_1$, respectively, $\mathbf{t}_1$ and $\mathbf{n}_1$ are expressed as:

$$\begin{aligned}\mathbf{t}_1 &= (1/\{1+[f'(x_1)]^2\}^{1/2},\ f'(x_1)/\{1+[f'(x_1)]^2\}^{1/2}),\\ \mathbf{n}_1 &= (-f'(x_1)/\{1+[f'(x_1)]^2\}^{1/2},\ 1/\{1+[f'(x_1)]^2\}^{1/2}).\end{aligned} \tag{12}$$

The position vector $\mathbf{R}_1$ directed from a point Q on the flagellum to the tip and position vector $\mathbf{R}_2$ directed from point Q to $R(x_2,f(x_2))$ between Q and the tip of the flagellum, were expressed as:

$$\begin{aligned}\mathbf{R}_1 &= (x_t-x_1,-f(x_1)),\\ \mathbf{R}_2 &= (x_2-x_1,f(x_2)-f(x_1)).\end{aligned} \tag{13}$$

If the speed of the medium is represented by V, the viscous resistance, C_NV, per unit length acts on each part of the flagellum (15). The bending moment, dM, around point Q on the flagellum due to the viscous resistance of the medium acting in a minute segment (length: ds_2) at point R is given by

$$dM=C_NV(\mathbf{R}_2,\mathbf{t}_1)ds_2. \tag{14}$$

Substituting Eqs. 12 and 13 into Eq. 14 and using $ds_2=\{1+[f'(x_2)]^2\}^{1/2}dx_2$ give the bending moment, dM,

$$\begin{aligned}dM=C_NV\{&x_2-x_1+[f(x_2)-f(x_1)]f'(x_1)\}\\ &\times\{1+[f'(x_2)]^2\}^{1/2}/\{1+[f'(x_1)]^2\}^{1/2}dx_2.\end{aligned} \tag{15}$$

Integrating the bending moment, dM, from the tip of the flagellum to Q gives the total bending moment $M(x_1)$ around point Q,

$$\begin{aligned}M(x_1)=C_NV\int_{x_t}^{x}&\{x_2-x_1+[f(x_2)-f(x_1)]f'(x_1)\}\\ &\times\{1+[f'(x_2)]^2\}^{1/2}/\{1+[f'(x_1)]^2\}^{1/2}dx_2.\end{aligned} \tag{16}$$

The total bending moment $M(x_1)$ is proportional to the slope $\theta_M(x_1)$ of the flagellum at point Q due to the bending of the flagellum.

$$\theta_M(x_1)=M(x_1)/S. \tag{17}$$

The deflection at the tip of the flagellum due to the bending of all segments is obtained by integrating the deflections due to all segments from the base to the tip of the flagellum:

$$\delta_B=\int_0^{x_t}(\mathbf{R}_1,\mathbf{t}_1)\theta_M(x_1)\{1+[f'(x_1)]^2\}^{1/2}dx_1. \tag{18}$$

The torsional moment, dT, around point Q due to the viscous resistance of the medium acting on a segment (length: ds_2) at point R is given by

$$dT=C_NV(\mathbf{R}_2,\mathbf{n}_1)ds_2. \tag{19}$$

Substituting Eqs. 12 and 13 into Eq. 19 and using $ds_2=\{1+[f'(x_2)]^2\}^{1/2}dx_2$ give the torsional moment, dT,

$$\begin{aligned}dT=C_NV&[(x_1-x_2)f'(x_1)+f(x_2)-f(x_1)]\\ &\times\{1+[f'(x_2)]^2\}^{1/2}/\{1+[f'(x_1)]^2\}^{1/2}dx_2.\end{aligned} \tag{20}$$

Integrating the torsional moment, dT, from the tip of the flagellum to Q gives the total torsional moment $T(x_1)$ around point Q on the flagellum,

$$\begin{aligned}T(x_1)=C_NV\int_{x_t}^{x_1}&[(x_1-x_2)f'(x_1)+f(x_2)-f(x_1)]\\ &\times\{1+[f'(x_2)]^2\}^{1/2}/\{1+[f'(x_1)]^2\}^{1/2}dx_2.\end{aligned} \tag{21}$$

The total torsional moment $T(x_1)$ is proportional to the angle of twist per unit length $\theta_T(x_1)$.

$$\theta_T(x_1)=T(x_1)/C, \tag{22}$$

where C is the torsional rigidity.

The deflection (δ_T) at the tip of the flagellum due to the torsion of all segments is obtained by integrating the deformation due to elementary segments from the base to the tip of the flagellum:

$$\delta_T=\int_0^{x_t}(\mathbf{R}_1,\mathbf{n}_1)\theta_M(x_1)\{1+[f'(x_1)]^2\}^{1/2}dx_1. \tag{23}$$

Assuming that Poisson's ratio is 0.5 (31), the flexural rigidity (S) is 1.5 times the torsional rigidity (C).

Adding the deflection due to bending and deflection due to torsion, and using $S=1.5C$, total deflection (δ) is given by

$$\begin{aligned}\delta=C_NV/S\{&\int_0^{x_t}\int_{x_t}^{x_1}[x_t-x_1-f(x_1)f'(x_1)][x_2-x_1+(f(x_2)-f(x_1))f'(x_1)]\\ &\times\{1+[f'(x_2)]^2\}^{1/2}/\{1+[f'(x_1)]^2\}^{1/2}dx_1dx_2\\ &+1.5\int_0^{x_t}\int_{x_t}^{x_1}[(x_1-x_2)f'(x_1)-f(x_1)][(x_1-x_2)f'(x_1)+f(x_2)-f(x_1)]\\ &\times\{1+[f'(x_2)]^2\}^{1/2}/\{1+[f'(x_1)]^2\}^{1/2}dx_1dx_2.\end{aligned} \tag{24}$$

Total deflection at the tip of the flagellum was obtained by loading the program containing Eq. 24 into the calculator and inputting the data, the distance x_t from the base to the tip, and the speed, V, of the stream of the medium, measured on the tracings of the beating flagellum.

Calculation of the flexural rigidity of motionless flagella. When a medium stream was applied in a direction perpendicular to the tangent at the base of the flagellum, the flagellum of the spermatozoon held by its head with the tip of a micropi-

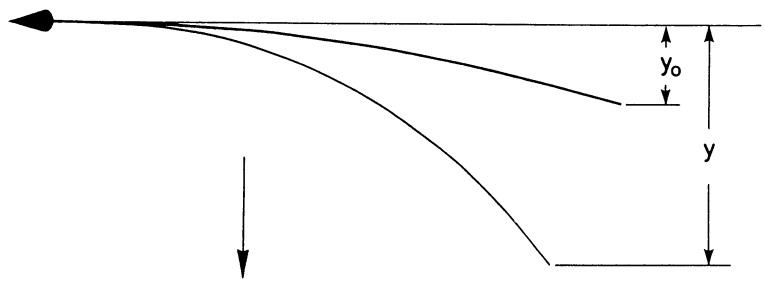

Fig. 7. The deformation of the motionless flagellum of a spermatozoon when a stream was applied in the direction at right angles to the tangent at the base of the flagellum. Arrows indicate the stream direction.

pette was bent by the viscous resistance of the medium acting on the flagellum (Fig. 7).

The deflection, $y-y_0$, of the flagellum at the tip by the viscous drag of the medium acting on all segments along the flagellum was numerically calculated for various values of flexural rigidity, assuming that the flagellum can be approximated by a series of circular arcs tangent to one another at their points of intersection (29). Values of previously mentioned drag coefficients, C_N, 2.7×10^{-3} Pa.s for ASW and 6.8×10^{-3} Pa.s for the reactivation solution and the ATP-free medium, were used in the present calculation. The flexural rigidity of motionless flagella was obtained by finding the value for flexural rigidity in which the calculated and observed deflections occur at the tip of the flagellum.

Calculation of the flexural rigidity of doublet microtubules. The principle of calculation of the flexural rigidity of doublet microtubules was the same as that of motionless flagella. Doublet microtubules attached to a coverslip at the proximal region were bent by the viscous resistance of the medium when a stream of medium was applied in a direction tangent to the base of the doublet microtubules. The flexural rigidity of doublet microtubules was calculated from the bend due to the stream and the viscous resistance caused by the stream. The coefficient of viscous resistance corrected for effects of the coverslip was calculated from Eq. 25,

$$C_N=4\pi\mu/\ln(2h/r), \tag{25}$$

where h is the distance of the microtubule from the coverslip, r is the radius of the microtubule, and μ is the viscosity of the medium, according to Katz and Blake (19). In the present study, the value 4.6×10^{-2} Pa.s was used for C_N, which was obtained by substituting the values h=25 nm, r=25 nm, and $\mu=2.5\times10^{-3}$ Pa.s, into Eq. 25. The distance of 25 nm from the coverslip was estimated from the relationship between the distance from the coverslip surface and the stream velocity (12). The estimation error in the hydrodynamic drag from the coverslip leads to an underestimation of the flexural rigidity by $<84\%$.

RESULTS

Flexural rigidity of beating flagella. The average flexural rigidity of flagella of *Clypeaster japonicus*, beating in the ASW was 4.2×10^{-22} Nm^2 (Table I). The average flexural rigidity of *Pseudocentrotus depressus* flagella was 4.6×10^{-22} Nm^2, which is similar to that of *Clypeaster japonicus*. The flexural rigidity of a single fla-

Table I. FLEXURAL RIGIDITY OF SAND DOLLAR SPERM FLAGELLA (10^{-21} Nm^2).

	Motionless flagella			Beating flagella				
	Medium		n	Medium	a*	n	b†	n
Live flagella	CO_2-saturated SW	11±6	(13)	Normal SW	0.42±0.31	(24)	5.8±2.6	(10)
	2 mM EHNA, ASW	0.19±0.04	(16)					
Demembranated flagella	0 mM ATP	14±4	(17)					
	2 μM ATP	15±8	(13)					
	1 mM ATP, 10 μM vanadate	0.31±0.15	(15)	1 mM ATP	1.0±0.6	(16)	12±3	(8)
	1 mM ATP, 2 mM EHNA	0.28±0.09	(12)					
Trypsin-digested demembranated flagella	0 mM ATP	16±5	(10)					
Doublet microtubules	0 mM ATP	0.061–0.23	(11)					
	0.1 mM ATP	0.014–0.38	(13)					

Mean±SD. Results from three to six experiments were averaged. n, number of spermatozoa measured.

* Bending in the beating plane.

† Bending in the direction perpendicular to the beating plane.

gellum was uniform at various regions along its entire length, except within the region approximately 5 μm from the base of the flagellum mentioned above. No significant difference was found in the flexural rigidity between measurements using the stream from the base to the tip of the flagellum "stretching" the flagellar wave and the stream from the tip to the base of the flagellum "compressing" the flagellar wave: $4.2 \pm 3.8 \times 10^{-22}$ Nm^2 for the stretched flagellar wave and $4.1 \pm 2.7 \times 10^{-22}$ Nm^2 for the compressed flagellar wave of *Clypeaster japonicus* spermatozoa (n=7).

The average flexural rigidity of beating flagella of *Clypeaster japonicus* for bending in the plane perpendicular to the beating plane was 5.8×10^{-21} Nm^2, which was 14 times that of beating flagella for bending within the beating plane (Table I). In *Pseudocentrotus depressus*, the average flexural rigidity for bending in the plane perpendicular to the beating plane was 7.1×10^{-21} Nm^2, which was 15 times that for bending within the beating plane.

Flexural rigidity of motionless live flagella. The flagellum of spermatozoon held by its head with the tip of a micropipette was bent by the viscous resistance of the medium acting on the flagellum when a medium stream was applied in the direction perpendicular to the tangent at the base of the flagellum.

In spermatozoa that had lost their motility in CO_2-ASW, the flagellum was slightly curved and its head was often tilted to the concave side of the flagellum (Fig. 8a and a′). When the spermatozoa were transferred to normal ASW, they swam along circular paths keeping the convex sides of the flagella to the centers of the circles as reported by Goldstein (14).

In *Clypeaster japonicus*, the average flexural rigidity of live flagella immobilized in CO_2-ASW was 1.1×10^{-20} Nm^2 when tested by bending within the beating plane (Table I). In *Pseudocentrotus depressus*, a similar value (1.3×10^{-20} Nm^2) was obtained. It was very difficult to bend the flagellum in the direction perpendicular to the "beating" plane, the plane in which the flagellum is expected to beat when the flagellum resumed moving, because the flagellum was twisted in many cases. In one case where the flagellum could be bent in the perpendicular plane, the flexural rigidity did not differ from that determined by bending the flagellum in the "beating" plane.

Flexural rigidity of demembranated flagella reactivated with ATP. The average flexural rigidity of reactivated demembranated flagella was 1.0×10^{-21} Nm^2 in *Clypeaster japonicus* (Table I) and 6.1×10^{-22} Nm^2 in *Pseudocentrotus depressus*. No difference was found between the flexural rigidity determined by "stretching" the flagellar wave by a stream flowing from the base to the tip of the flagellum and that determined by "compressing" from the stream in opposite direction.

The average flexural rigidity of reactivated flagella for bending in the plane perpendicular to the beating plane was 1.2×10^{-20} Nm^2, which was 12 times that of

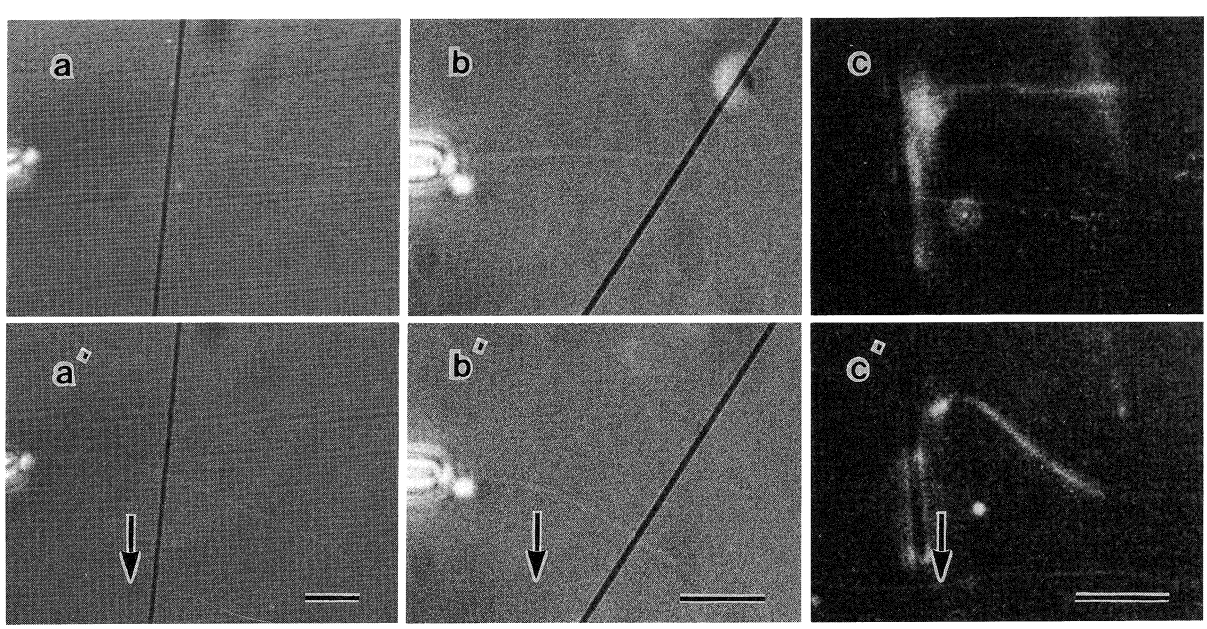

Fig. 8. Changes in the form of the flagellum (a, a′, b, and b′) and doublet microtubules (c and c′) of a spermatozoon by the medium stream. a, b, and c are in still medium and a′, b′, and c′ are in the medium moving in the direction indicated by the arrows. The stream velocity is 160 μm/s in a′, 200 μm/s in b′ and 38 μm/s in c′. a and a′ are live flagella in CO_2-ASW, and b and b′ are demembranated flagella in ATP-free medium. The scale bar represents 10 μm in a′ (for a and a′) and b′ (for b and b′) and 5 μm in c′ (for c and c′).

reactivated flagella for bending within the beating plane in *Clypeaster japonicus* (Table I) and 1.0×10^{-20} Nm^2, which was 17 times that of beating flagella for bending within the beating plane in *Pseudocentrotus depressus*. It is noted that the values of flexural rigidity in reactivated flagella are similar to those in intact beating flagella.

Flexural rigidity of motionless demembranated flagella. The flexural rigidity of demembranated flagella obtained by treating normal flagella with Triton X-100 was measured in ATP-free medium (Fig. 8b and b′) and in medium containing 2 μM ATP. The average flexural rigidity of motionless demembranated flagella was 1.4×10^{-20} Nm^2 in ATP-free medium and 1.5×10^{-20} Nm^2 in medium containing 2 μM ATP in *Clypeaster japonicus* (Table I).

Effects of vanadate on the flexural rigidity of demembranated flagella. Demembranated spermatozoa beating in reactivation solution containing 1 mM ATP were put into solutions containing various amounts of sodium vanadate and 1 mM ATP. In the presence of vanadate, up to 2 μM, the beat frequency decreased, while other parameters were scarcely changed. When the vanadate concentration exceeded 2 μM, some nonmotile spermatozoa were noticed. The sperm flagella, which were immobilized by 3 to 4 μM vanadate, were slightly curved along their length and rather straight in solutions containing 5 μM or more vanadate.

The average flexural rigidity of motionless demembranated flagella in the medium containing 1 mM ATP and 10 μM vanadate was 3.1×10^{-22} Nm^2, which is only two percent of that of motionless demembranated flagella in ATP-free medium and similar to that of beating flagella for bending within the beating plane (Table I). No difference in flexural rigidity was found for the measurements by bending in one plane and bending in the perpendicular to the former.

Effects of EHNA on the flexural rigidity of flagella. Spermatozoa beating in ASW were put into solutions containing various concentrations of EHNA. EHNA caused no change in flagellar movement when the concentration was less than 0.5 mM. When EHNA concentrations exceeded 0.5 mM, a few nonmotile spermatozoa were noticed in the sample, and fifty percent of the spermatozoa became immotile with 2 mM EHNA. The average flexural rigidity of motionless live flagella poisoned with 2 mM EHNA was 1.9×10^{-22} Nm^2 (Table I).

Demembranated spermatozoa beating in reactivation solution containing 1 mM ATP were put into solutions containing various concentrations of EHNA and 1 mM ATP. The effects of EHNA on demembranated flagella were similar to that of EHNA on live flagella: EHNA, up to 0.5 mM, caused no effect on flagellar movement. When the EHNA concentration increased, the beat frequency of flagella decreased, while the other wave parameters remained unchanged or slightly changed. Fifty percent inhibition in the sample was obtained using 2 mM EHNA.

The average flexural rigidity of motionless demembranated flagella in the medium containing 1 mM ATP and 2 mM EHNA was 2.8×10^{-22} Nm^2, which was similar to that of motionless demembranated flagella in the medium containing 10 μM sodium orthovanadate (Table I).

Flexural rigidity of trypsin-digested demembranated flagella. The demembranated flagella, which had been treated with a solution containing 100 μg/ml trypsin for 5 min and held by sucking its proximal region into a micropipette, was bent when a stream of the medium was applied. The average flexural rigidity of demembranated flagella digested with trypsin in ATP-free medium was 1.6×10^{-20} Nm^2, which was similar to that of live flagella immobilized in CO_2-ASW (Table I).

Flexural rigidity of doublet microtubules. Doublet microtubules were obtained by disintegrating the trypsin-digested demembranated flagella with 1 mM ATP. Doublet microtubules attached to the coverslip at one end were bent when a stream of medium was applied in the direction perpendicular to the tangent at the attached end of the microtubules (Fig. 8c and c′). The flexural rigidity of doublet microtubules was $6.1\text{–}23 \times 10^{-23}$ Nm^2 in ATP-free medium and $1.4\text{–}38 \times 10^{-23}$ Nm^2 in a medium containing 0.1 mM ATP (Table I).

DISCUSSION

To determine the flexural rigidity of sperm flagella, we assumed that the difference in the waveform of the flagellum is due to the elastic deformation of the beating flagellum caused by the difference in the movement of the medium. As shown in Fig. 3, both the beat frequency and the wave number were practically unchanged by the stream when the speed was smaller than a definite value (280 μm/s in the case of Fig. 3). Beat frequency is directly proportional to the number of dynein arms, which are responsible for generating the sliding movements between doublet microtubules (11). Therefore, it seems likely that the process of active force generation in beating flagella is not affected by the stream of the medium within the above range.

The flexural rigidity of flagella determined in the present study are similar to those of demembranated flagella in ATP-free medium (1.1×10^{-20} Nm^2 for *Hemicentrotus pulcherrimus*) obtained by Okuno and Hiramoto (26) and those in the medium containing 10 μM vanadate and 1 mM ATP (8.9×10^{-22} Nm^2 for *Lytechinus pictus*) obtained by Okuno (25). However, in live flagella immobilized in CO_2-ASW, the flexural rigidity in the present study (1.1×10^{-20} Nm^2) is larger than that ($0.3\text{–}1.5 \times 10^{-21}$ Nm^2) obtained by Okuno and Hiramoto (26). According to Brokaw and Simonick (6) and

Brokaw (5), CO_2 causes direct inhibition of the bend angle without affecting frequency, while the change in ATP concentration causes large changes in the beat frequency and only slight changes in wavelength and amplitude of the bending waves. They also showed that spermatozoa suddenly stop moving and retain a "rigor wave" configuration when suddenly exposed to a relatively high CO_2 concentration, similar to those obtained by a sudden reduction in ATP concentration (12), whereas the spermatozoa reduce their movement and eventually stop showing nearly straight configurations at low CO_2 concentrations. Since the spermatozoa were suddenly put into CO_2-ASW containing a high CO_2 concentration in the present study, it is possible that the spermatozoa were in a "rigor" state, and consequently, had a high stiffness. Flexural rigidity of doublet microtubules obtained by disintegrating the trypsin-digested demembranated flagella with ATP was determined from their bending due to the stream of the surrounding medium. The wide variation in the rigidity values (Table I) may be due to variation in the number of doublet microtubules contained in fibers used in the experiment. Minimum values (1.4×10^{-23} Nm^2 in medium containing 0.1 mM ATP and 6.1×10^{-23} Nm^2 in ATP-free medium) may indicate the rigidity of single doublet microtubules. These values are reasonable because the mean flexural rigidity of taxol-stabilized microtubules is 2.2×10^{-23} Nm^2 (13).

It is noted in Table I that values of the flexural rigidity of demembranated flagella in ATP-free medium and that in medium containing 2 μM ATP are more or less the same as the value for live flagella immobilized with CO_2-ASW, suggesting that the cell membrane makes a minor contribution to the rigidity of the flagellum. It is also noted that the flexural rigidity of demembranated flagella is scarcely affected by digestion with trypsin that removes the radial spokes and nexin links. This fact suggests that spokes and nexin links make minor contributions to the flexural rigidity of the axoneme. Gibbons and Gibbons (12) reported that digestion of the rigor wave of the axoneme with trypsin to an extent sufficient to destroy most of the spokes and nexin links has no effect on the form of the rigor wave.

As reported by Okuno and Hiramoto (26), the stiffness of demembranated flagella is decreased with the addition of ATP and becomes equivalent to that of live ones in the medium containing 10 mM ATP. As already mentioned, the flexural rigidity of motionless flagella immobilized with EHNA and vanadate, which inhibit dynein-ATPase activity, was only several percent of that of motionless demembranated flagella in ATP-free medium. Since the flagellum is in a relaxed state in the presence of $MgATP^{2-}$ and vanadate (25), these results suggest that the flexural rigidity of the flagellum is mainly due to the microtubules connected with dynein arms.

The flexural rigidity for the bending with the beating plane is far smaller than that for the bending in the plane perpendicular to the beating plane in live beating flagella. Similar results were obtained in demembranated flagella reactivated with ATP. In both cases, the flagellum is more than ten times more flexible for the bending within the beating plane compared with that for the bending in the perpendicular plane. Values of the flexural rigidity in beating demembranated flagella determined by bending in the direction perpendicular to the beating plane were somewhat the same as those in live motionless flagella in CO_2-ASW, demembranated flagella in ATP-free or 2 μM ATP medium, and trypsin-digested demembranated flagella. The flexural rigidity of beating flagella for the bending within the beating plane was similar to those of motionless flagella immobilized with EHNA or vanadate. These facts suggest that the difference in the flexural rigidity from the difference in bending directions is due to the difference in the dynein cross-bridges formed between adjacent doublet microtubules in different doublet couples; the number of dynein cross-bridges in the direction at right angles to the beating plane is larger than that of dynein cross-bridges parallel to the beating plane.

There was little difference in flexural rigidity of the beating flagellum for bending within the beating plane between measurements by stretching the flagellar wave and compressing it. This fact implies that the contribution to flexural rigidity of other shear-resistant links such as nexin links and radial spokes is insignificant in beating flagellum as well. This is in disagreement with the prediction by Blum and Hines (2) that the contribution to stiffness of the nexin links or radial spokes is essential, but Warner (33) and Bozkurt and Woolley (4) concluded from their observation using an electron microscope that the nexin links were inextensible. Thus, the nexin links cannot act as an elastic resistance to movement.

The flexural rigidity for bending in the plane perpendicular to the beating plane was obtained using Eq. 24 assuming that the axonemes were homogeneous isotropic materials; the ratio of the flexural rigidity (S) to the torisional rigidity (C) is 1.5. The axonemes, however, have complex structures; such fibers may have different elastic properties between the directions parallel to the long axis and perpendicular to it. The values of S/C are calculated to be 5.4 for silk and 3.4 for wool from experimental data (8, 24). Using $S/C = 5.4$, the values of the flexural rigidity for bending in the plane perpendicular to the beating plane can be 3.6 times the values shown in Table I, because the flexural rigidity varies maximally by a factor, S/1.5C.

Young's modulus of the doublet microtubule is calculated from its flexural rigidity and the second moment of its cross section. The latter is calculated to be $3.8 \times$

10^{-32} m^4, assuming that both the A- and B-tubules have an elliptical cross section with 5 nm wall thickness, with the outer diameter of the cross section of the A-tubule being 25 nm in major axis and 23 nm in minor axis, and the outer diameter of the cross section of the B-tubule being 29 nm in major axis and 22 nm in minor axis (34). Young's modulus of microtubules was estimated to be 3.7×10^8 Pa from the lowest values of the flexural rigidity of the doublet microtubule in the present study (1.4×10^{-23} Nm^2). This value for Young's modulus is reasonable for a protein fiber, e.g., Young's modulus for flagellin of bacterial flagella (9) is 10^{10} Pa, the order for F-actin of striated muscles is 10^{10} Pa (27), the order for collagen is 10^9 Pa (23), and the order for silk is 10^8–10^{10} Pa (35).

Acknowledgments. We thank the Misaki Marine Biological Station of the University of Tokyo for supplying materials. We also thank Drs. Y. Hamaguchi, M. Okuno, and S.A. Baba for thier active interest and advice.

REFERENCES

1. Baba, S.A. 1972. Flexural rigidity and elastic constant of cilia. *J. Exp. Biol.,* **56**: 459–467.
2. Blum, J.J. and Hines, M. 1979. Biophysics of flagellar motility. *Quart. Rev. Biophys.,* **12**: 103–180.
3. Bouchard, P., Penningroth, S.M., Cheung, A., Gagnon, C., and Bardin, C.W. 1981. erythro-9-[3-(2-Hydroxynonyl)] adenine is an inhibitor of sperm motility that blocks dynein ATPase and protein carboxymethylase activities. *Proc. Natl. Acad. Sci. USA,* **78**: 1033–1036.
4. Bozkurt, H.H. and Woolley, D.M. 1993. Morphology of nexin links in relation to interdoublet sliding in the sperm flagellum. *Cell Motil. Cytoskel.,* **24**: 109–118.
5. Brokaw, C.J. 1977. CO_2-inhibition of the amplitude of bending of triton-demembranated sea urchin sperm flagella. *J. Exp. Biol.,* **71**: 229–240.
6. Brokaw, C.J. and Simonick, T.F. 1976. CO_2 regulation of the amplitude of flagellar bending. In *Cell Motility* (R. Goldman, T. Pollard, and T. Rosenbaum, eds.). Cold Spring Harbor Laboratory, New York, pp 933–940.
7. Fagan, J.B. and Racker, E. 1977. Reversible inhibition of (Na^+, K^+) ATPase by Mg^{2+}, adenosine triphosphate, and K^+. *Biochemistry,* **16**: 152–158.
8. Finlayson, D. 1946. Yarns for special purposes—effect of filament size. *J. Text. Inst.,* **37**: P168–P180.
9. Fujime, S., Maruyama, M., and Asakura, S. 1972. Flexural rigidity of bacterial flagella studied by quasielastic scattering of laser light. *J. Mol. Biol.,* **68**: 347–359.
10. Gibbons, B.H. and Gibbons, I.R. 1972. Flagellar movement and adenosine triphosphate activity in sea urchin sperm extracted with Triton X-100. *J. Cell Biol.,* **54**: 75–97.
11. Gibbons, B.H. and Gibbons, I.R. 1973. The effect of partial extraction of dynein arms of the movement of reactivated sea urchin sperm. *J. Cell Sci.,* **13**: 337–358.
12. Gibbons, B.H. and Gibbons, I.R. 1974. Properties of flagellar rigor waves formed by abrupt removal of adenosine triphosphate from actively swimming sea urchin sperm. *J. Cell Biol.,* **63**: 970–985.
13. Gittes, F., Mickey, B., Nettleton, J., and Howard, J. 1993. Flexural rigidity of microtubules and actin filaments measured from thermal fluctuations in shape. *J. Cell Biol.,* **120**: 923–934.
14. Goldstein, S.F. 1979. Starting transients in sea urchin sperm flagella. *J. Cell Biol.,* **80**: 61–68.
15. Gray, J. and Hancock, G.J. 1955. The propulsion of sea-urchin spermatozoa. *J. Exp. Biol.,* **32**: 802–814.
16. Hiramoto, Y. 1974. A method of microinjection. *Exp. Cell Res.,* **87**: 403–406.
17. Ishijima, S., Oshio, S., and Mohri, H. 1986. Flagellar movement of human spermatozoa. *Gamete Res.,* **13**: 185–197.
18. Johnston, D.N., Silvester, N.R., and Holwill, M.E.J. 1979. An analysis of the shape and propagation of waves on the flagellum of *Crithidia oncopelti. J. Exp. Biol.,* **80**: 299–315.
19. Katz, D.F. and Blake, J.R. 1975. Flagellar motions near walls. In *Swimming and Flying in Nature* Vol. 1 (T.Y.-T. Wu, C.J. Brokaw, and C. Brennen, eds.). Plenum Press, New York, pp 173–184.
20. Landau, L.D. and Lifshitz, E.M. 1986. *Theory of Elasticity.* 3rd English ed. Pergamon Press, London.
21. Lighthill, J. 1976. Flagellar hydrodynamics. *SIAM Rev.,* **18**: 161–230.
22. Machin, K.E. 1958. Wave propagation along flagella. *J. Exp. Biol.,* **35**: 796–806.
23. Mason, P. 1965. The viscoelasticity and structure of keratin and collagen. *Kolloid-Z. Z. Polym.,* **202**: 139–147.
24. Meredith, R. 1954. The torsional rigidity of textile fibres. *J. Text. Inst.,* **45**: T489–T503.
25. Okuno, M. 1980. Inhibition and relaxation of sea urchin sperm flagella by vanadate. *J. Cell Biol.,* **85**: 712–725.
26. Okuno, M. and Hiramoto, Y. 1979. Direct measurements of the stiffness of echinoderm sperm flagella. *J. Exp. Biol.,* **79**: 235–243.
27. Oosawa, F. 1980. The flexibility of F-actin. *Biophys. Chem.,* **11**: 443–446.
28. Rikmenspoel, R. and Isles, C.A. 1985. Digitized precision measurements of the movements of sea urchin sperm flagella. *Biophys. J.,* **47**: 395–410.
29. Seames, A.E. and Conway, H.D. 1957. Numerical procedure for calculating the large deflections of straight and curved beams. *J. Appl. Mech.,* **24**: 289–294.
30. Summers, K.E. and Gibbons, I.R. 1971. Adenosine Triphosphate-induced sliding of tubules in trypsin-treated flagella of sea-urchin sperm. *Proc. Natl. Acad. Sci. USA,* **68**: 3092–3096.
31. Wainwright, S.A., Biggs, W.D., Curray, J.D., and Gosline, J.M. 1982. *Mechanical Design in Organisms.* Princeton University Press, Princeton.
32. Warner, F.D. 1974. The fine structure of the ciliary and flagellar axoneme. In *Cilia and Flagella* (M.A. Sleigh, ed.). Academic Press, London, pp 11–37.
33. Warner, F.D. 1983. Organization of interdoublet links in Tetrahymena cilia. *Cell Motil.,* **3**: 321–332.
34. Warner, F.D. and Satir, P. 1973. The substructure of ciliary microtubules. *J. Cell Sci.,* **12**: 313–326.
35. Whittaker, E.T. and Robinson, G. 1926. *The Calculus of Observations.* 2nd ed. Blackie and Son, London.

(Received for publication, May 31, 1994
and in revised form, June 21, 1994)